Formation of Supported Phospholipid Bilayers from Unilamellar Vesicles Investigated by Atomic Force Microscopy

Ilya Reviakine and Alain Brisson*

Department of Biophysical Chemistry, GBB, University of Groningen, Nijenborgh 4, 9747 AG Groningen, The Netherlands

Received March 16, 1999. In Final Form: September 16, 1999

Since their introduction through the work of McConnell et al. in the early 80s, supported phospholipid bilayers (SPBs) have proven to be a versatile model system for investigating a wide variety of phenomena. Despite their continuous application in fundamental as well as applied research fields, the mechanism by which SPBs are formed from suspensions of unilamellar vesicles remains poorly understood. Utilizing the ability of atomic force microscopy (AFM) to investigate processes in situ and in real time, we have studied the early stages of SPB formation on mica. Unilamellar vesicles of various sizes, composed of zwitterionic phospholipids, were prepared by sonication or extrusion. Vesicles of all sizes investigated were found to adsorb to mica. Unruptured vesicles forming supported vesicular layers (SVLs), as well as disks, formed as a result of vesicle rupture, could be visualized by AFM. The behavior of the SVLs was found to depend on the vesicle size, the lipid concentration, and the presence or absence of Ca^{2+}. The picture of the mechanism of SPB formation, which emerges from the results presented in this report, is critically compared with theoretical predictions and experimental results reported to date.

Introduction

The preparation of protein-incorporating supported phospholipid bilayers (SPBs) by fusion of unilamellar vesicles on solid supports was pioneered by the group of McConnell[1] for studying cell−cell interaction processes. Due to their unique properties, SPBs prepared in this fashion (Figure 1a) have subsequently found applications in fundamental (from structural biology to physics) as well as applied (surface modification, biosensor technology) research fields.[2,3] New methods of preparation of SPBs by vesicle fusion (VF) keep appearing[3−5]—a clear indication that their use in various disciplines will continue to flourish.

Aspects of SPB formation by vesicle fusion on hydrophilic and hydrophobic surfaces have been investigated by a variety of techniques.[3,5,6−10] Several important factors affecting the process were identified—the lipid composition of vesicles[8] and the concentration of monovalent and divalent cations[3,7,8]—and hypotheses concerning the mechanism of SPB formation by vesicle fusion have been advanced.[2,9,11] However, no consistent picture has yet emerged. Arguments concerning the "stressed" nature of sonicated unilamellar vesicles (SUVs), which are commonly used to prepare SPBs, are put forward whenever the driving forces for SPB formation are discussed—despite abundant evidence that SPBs can be formed equally well from vesicles obtained by extrusion and dialysis[1,3,8,12] (Table 1). A theoretical framework describing the behavior of vesicles, including their adhesion to surfaces, fusion of surface-bound vesicles, and their rupture, has been elaborated by Seifert and Lipowsky,[13,14] but comparison with experimental studies of SPB formation is lacking.

SPBs are attractive to the bio-scanning probe microscopy (SPM) community as substrates for binding and imaging proteins, DNA, and other macromolecules. They have therefore become the object of investigations by AFM at the early stages of biological SPM (see, for example, reviews by Shao et al.[15,16]) and have recently been used in our group to support the growth of two-dimensional (2D) protein crystals.[17] A typical AFM image of an SPB is presented in Figure 1b. Such a structure forms when unilamellar vesicles are deposited on a suitable surface under a wide variety of conditions.

In this report we present several new features of the process of SPB formation from unilamellar vesicles on mica revealed by AFM and analyze the results in terms of the theoretical framework of Seifert and Lipowsky.[13,14]

Experimental Section

The lipids used in this study—99% pure egg yolk phosphatidylcholine (EggPC), dioleoyl phosphatidylcholine (DOPC), dioleoyl phosphatidylserine (DOPS)—were purchased from Avan-

* Corresponding author. Phone: 31 50 363 42 16. Fax: 31 50 363 48 00. E-mail: brisson@chem.rug.nl.

(1) Watts, T. H.; Brian, A. A.; Kappler, J. W.; Marrack, P.; McConnell, H. *Proc. Natl. Acad. Sci. U.S.A.* **1984**, *81*, 7564. Watts, T. H.; Gaub, H. E.; McConnell, H. M. *Nature* **1986**, *320*, 179.
(2) Sackmann, E. *Science* **1996**, *271*, 43.
(3) Kalb, E.; Frey, S.; Tamm, L. K. *Biochim. Biophys. Acta* **1992**, *1103*, 307.
(4) Brink, G.; Schmitt, L.; Tampe, R.; Sackmann, E. *Biochim. Biophys. Acta* **1994**, *1196*, 227.
(5) Cheng, Y.; Boden, N.; Bushby, R.; Clarkson, S.; Evans, S. D.; Knowles, P. F.; Marsh, A.; Miles, R. *Langmuir* **1998**, *14*, 839.
(6) Bayerl, T. M.; Bloom, M. *Biophys. J.* **1990**, *58*, 357.
(7) Müller, D. J.; Amrein, M.; Engel, A. *J. Struct. Biol.* **1997**, *119*, 172.
(8) Nollert, P.; Kiefer, H.; Jähnig, F. *Biophys. J.* **1995**, *69*, 1447.
(9) Keller, C. A.; Kasemo, B. *Biophys. J.* **1998**, *75*, 1397.
(10) Keller, C. A.; Glasmaester, K.; Zhdanov, V. P.; Kasemo, B. Paper presented at the Centennial Meeting of the American Physical Society, March 1999, Atlanta, GA. *Bull. Am. Phys. Soc.* **1999**, *44* (1) *Part II*, 1936. Manuscript submitted for publication.
(11) Benz, J.; Düzgünes, N.; Nir, S. *Biochemistry* **1983**, *22*, 3320.
(12) Reviakine, Mazères, Simon, and Brisson. Unpublished observations.
(13) Seifert, U. *Adv. Phys.* **1997**, *46*, 13.
(14) Lipowsky, R.; Seifert, U. *Mol. Cryst. Liq. Cryst.* **1991**, *202*, 17.
(15) Shao, Z.; Mou, J.; Czajkowsky, D. M.; Yang, J.; Yuan, J.-Y. *Adv. Phys.* **1996**, *45*, 1.
(16) Shao, Z.; Yang, J.; Somlyo, A. P. *Annu. Rev. Cell Dev. Biol.* **1995**, *11*, 241.
(17) Reviakine, I.; Bergsma-Schutter, W.; Brisson, A. *J. Struct. Biol.* **1998**, *121*, 356.

10.1021/la9903043 CCC: $19.00
Published on Web 01/21/2000

Table 1. Conditions for SPB Formation on Hydrophilic Surfaces[a]

substrate	lipid	vesicles	buffer composition	result	ref.
mica	DPPC	SUVs[b]	20 or 170 mM NaCl	SPB[c]	20, 41, 42
glass	EggPC + cholesterol	DUVs[d] + protein	140 mM NaCl in 10 mM Tris, pH 8	SPB	1
quartz	POPC	EUVs[e]	150 mM NaCl, 10 mM Tris, pH 7.4	SPB	3
	POPC/POPG	70−90 nm	100 mM Na_3SO_4, 10 mM HEPES, pH 7.4		8
glass, quartz, SiO_2,[g] Si_3N_4	*E. coli*	EUVs, 75−90 nm	100 mM Na_3SO_4, 10 mM HEPES, pH 7.4	SVL[f]	8
	E. coli		100 mM Na_3SO_4, 20 mM Ca^{2+}, 10 mM HEPES, pH 7.4	SPB	8
Al_2O_3	POPC		100 mM Na_3SO_4, 10 mM HEPES, pH 7.4	N.F.[h]	8
glass (beads)	DMPC	SUVs	water	SPB	6
SiO_2[i]	DOPC/DOPS	SUVs	100 mM NaCl, 3 mM Ca^{2+} in 10 mM Tris, pH 7.5	SPB	50
	EggPC	SUVs	100 mM NaCl, 10 mM Tris, pH 8	SPB	9

[a] The conditions presented are taken directly from the references listed. Only the results pertinent to this report were included. [b] SUVs, sonicated unilamellar vesicles. [c] SPB, supported phospholipid bilayer. [d] DUVs, unilamellar vesicles obtained by detergent dialysis. [e] EUVs, unilamellar vesicles obtained by extrusion. [f] SVL, supported vesicular layer.[8] [g] N.F., no fusion was observed. [h] Oxidized silicon wafers. [i] A 100 nm layer of SiO_2 evaporated onto a support.[9]

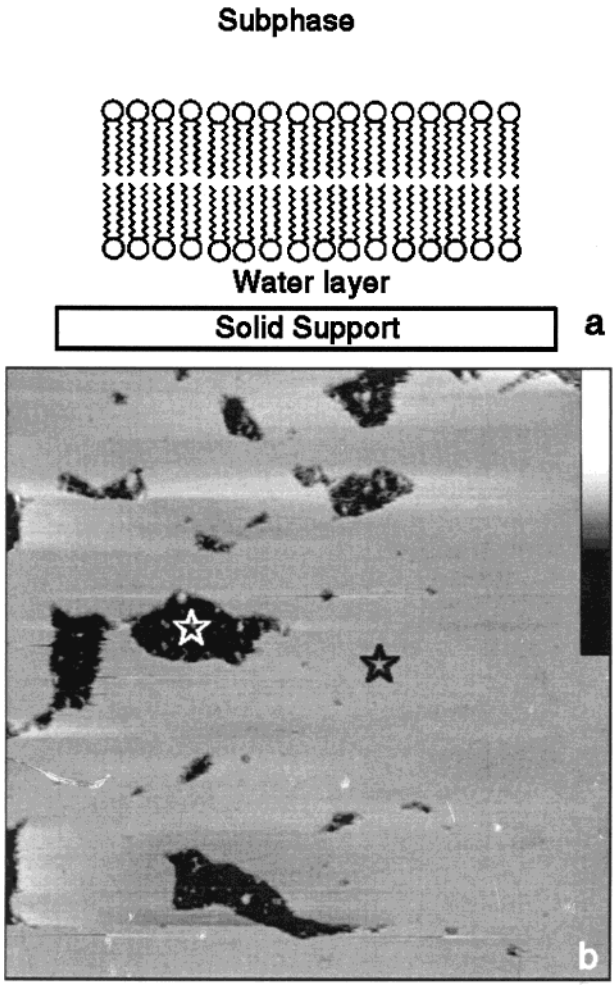

Figure 1. (a) Schematic representation of a supported phospholipid bilayer, as viewed from the side. The bilayer is separated from the solid support by an ultrathin layer of water or buffer, which was used to prepare the vesicles.[2] (b) Typical contact-mode constant-force AFM image of an incompletely formed SPB. Several defects (which would disappear if the process were allowed to go to completion) are visible, and two levels—mica (white star) and the lipid (~3.5 nm higher than the mica, black star)—are clearly distinguishable. Image size: 3 μm. *Z*-scale: 10 nm.

ti Polar Lipids (Alabaster, AL). Monosialoganglioside (G_{M1}) and cholera toxin subunit B_5 (CTB_5) were purchased from Sigma (St. Louis, MO). Other chemicals were purchased from Merk (Germany) or Sigma. Water used throughout this study was purified with a MilliQ water purification system (Millipore). All glassware used in this study was stored overnight in a mixture of chromic and sulfuric acids (Merk, Germany) and rinsed thoroughly with water prior to use.

Silicon wafers were boiled in $NH_4OH/H_2O_2/H_2O$, washed with water, boiled in $HCl/H_2O_2/H_2O$, and finally extensively rinsed with water prior to use.[18] After such a washing procedure, the contact angle of water is typically <10°.

Buffers contained (1) 2 mM EDTA, 10 mM HEPES, pH 7.4; (2) 40 mM NaCl, 2 mM EDTA, 10 mM HEPES, pH 7.4; (3) 20 mM NaCl in water; (4) 2 mM $CaCl_2$, 150 mM NaCl, 10 mM Hepes, 3 mM NaN_3, pH 7.4; (5) 2 mM EDTA, 150 mM NaCl, 10 mM HEPES, 3 mM NaN_3, pH 7.4; and (6) 2 mM $CaCl_2$, 40 mM NaCl, 10 mM HEPES, pH 7.4. All buffers were filtered through a 200 nm syringe filter (Schleicher and Schuell, Germany) prior to use.

Multilamellar vesicles (MLVs) were obtained by mixing appropriate amounts of lipids dissolved in chloroform or chloroform/methanol (2:1 v/v) and evaporating the solvent with argon. After a further 30−40 min of drying in a desiccator connected to a rotary vacuum pump, the lipids were resuspended by vortexing in an appropriate buffer at the concentration required. SUVs were produced from the MLV suspension by sonication to clarity (ca. ~45 min, in pulsed mode at 30% duty cycle), during which the suspension was kept in an ice bath, with a tip sonicator (Brandson Ultrasonics Corp., Danbury, CT). Extruded unilamellar vesicles (EUVs) were obtained from the MLVs by extrusion through filters of appropriate pore diameters using a Lipofast extruder (Avestin, Inc., Canada).

One hundred microliters of freshly prepared unilamellar vesicles were deposited onto a cleaved mica surface and incubated for 5−60 min at room temperature. The excess of vesicles was removed by exchanging the solution covering the mica with a buffer (this is referred to in Table 2 as "Wash"), and the sample was installed in the atomic force microscope. The microscope was allowed to thermally equilibrate for a minimum of 30 min before imaging.

In situ SPB formation was performed in one of two ways: a freshly cleaved piece of mica was installed in the microscope, and after allowing the microscope to equilibrate for a minimum of 30 min, a freshly sonicated EggPC suspension diluted to 8 μg/mL in buffer (4) was either (i) continuously infused using a syringe pump (Model A-99, Razel Scientific Instruments, CT) or (ii) injected 0.1 mL at a time.

Binding of CTB_5 to mica was induced by injecting a 25 μg/mL CTB_5 solution in an appropriate buffer into the fluid cell. Although CTB_5 molecules were visible in the defectuous areas of the SPBs almost immediately after injection, the contrast improved significantly after exchanging a calcium-containing buffer for a buffer without calcium.

AFM observation was performed using a Nanoscope IIIa-MultiMode atomic force microscope (Digital Instruments, Santa Barbara, CA) equipped with a "J" (120 μm) scanner. The contact mode fluid cell (Digital Instruments) was washed extensively with water, with 95% ethanol, and again with water before each experiment. O-rings, washed overnight in a 1% Helmanex solution (GMBH, Germany) and sonicated three times in

(18) Tiberg, F.; Landgren, M. *Langmuir* **1993**, *9*, 927.

Table 2. Summary of the Experimental Conditions Used and the Results Obtained in This Study

substrate	vesicles	starting solution[a]	wash	result
mica	SUVs[b]	EggPC or DOPC, Buf 1, 2, or 3	1, 2, or 3	no fusion; vesicles
		EggPC or DOPC, Buf 1, 2, or 3	4 or 6	fusion; SPB[d]
		EggPC or DOPC, Buf 4	any	fusion; SPB
		1 mg/mL EggPC, Buf 5	5	SPB; defects
		DOPC/G_{M1}, Buf 4	any	fusion; SPB
		DOPC/DOPS, Buf 4	any	fusion; SPB
	EUVs[c] 30 or 50 nm	up to 3 mg/mL EggPC, Buf 5	5	vesicles;[51] no SPB
		0.001−0.1 mg/mL EggPC, Buf 4	4	vesicles; disks; SPB; defects
	EUVs, 100 nm	0.006 mg/mL EggPC, Buf 4	4	disks; vesicles
		0.06 mg/mL EggPC, Buf 5	5	vesicles + disks (Figure 3)
	EUVs, 200 nm	1.5 mg/mL EggPC, Buf 4	4	SPB
		3 mg/mL eggPC, Buf 5	5	disks
SiO_2	SUVs	EggPC, Buf 1	1	fusion; SPB

[a] Compositions of buffers are listed in the Experimental Section. [b] A lipid concentration of 0.5 mg/mL was used in experiments involving SUVs, unless otherwise indicated. [c] The pore radius of the membranes through which the liposome suspension was extruded is quoted for the EUVs. [d] Once formed, an SPB is insensitive to buffer exchange.

ultrapure water, were used in experiments where buffer exchange or continuous infusion was required. Mica plates (12 mm in diameter, Metafix, Montdidier, France) were glued to the Teflon adhesive tape ("BYTAC", Norton Performance Plastics Corporation, Akron, OH)-coated metal disks using Rapid epoxy glue (according to the procedure described in ref 7). Clean ~1 × 1 cm^2 silicon wafers were glued onto metal disks using double-sided tape.

Images were recorded in the constant-force mode using oxide-sharpened silicon nitride tips mounted on cantilevers with nominal force constants of 0.06 N/m, at scanning rates of 8−15 Hz.[19] The scan angle was 90°. The force was kept at the lowest possible value by continuously adjusting the set point during imaging. Images were flattened and plane-fitted as required.

Results

Cholera Toxin Subunit B (CTB_5) as a Tool To Investigate SPB Formation by AFM. Mou et al. have shown that CTB_5 adsorbs to mica but not to lipid bilayers lacking G_{M1}.[20] Figure 2a shows CTB_5 molecules adsorbed to the mica surface exposed in a defectuous area of an SPB. The average height of CTB_5 molecules (3.5 nm[21]) is 1 ± 0.1 nm ($n = 12$) lower than that of the surrounding lipid domains, as is expected for lipid domains consisting of a single lipid bilayer. In the experiments which are discussed below (summarized in Table 2), CTB_5 was used to test for the presence of an SPB.

SPB Formation versus Vesicle Adsorption. Effect of Ca^{2+} and Vesicle Size. The following definitions are provided to clarify the subsequent material. "Adsorption" refers to the transition between a vesicle in solution (a free vesicle) and an intact vesicle bound to a surface. "Rupture" refers to the transition between an adsorbed, intact vesicle and an adsorbed, single-bilayer disk. In this context "intact" means "unruptured". "Fusion" is used to signify the formation of a larger vesicle, free or bound, from two or more smaller vesicles, free or bound. "Coalescence" refers to joining of single-bilayer disks. The influence of the vesicle size and of the preparation method on SPB formation was tested with vesicles prepared either by sonication (SUVs) or by extrusion (EUVs). All results discussed below are summarized in Table 2.

SUVs ($R \sim 12$ nm[22]). An alternative to the formation of an SPB is the formation of a supported vesicular layer (SVL). This phenomenon has first been reported by Nollert et al. with SUVs made of *Escherichia coli* lipid extract[23] in the absence of Ca^{2+}, while an SPB was formed upon addition of Ca^{2+} (Table 1).[8] Keller et al.[9,10] have recently reported that adsorption of EggPC SUVs precedes the formation of an SPB on silicon oxide (Table 1), thus suggesting that absorption of SUVs is a general phenomenon, not restricted to a particular class of lipids.[23] We found that SUVs prepared in EDTA-containing buffers (up to ~0.5 mg/mL of lipid) adsorbed to mica intact, forming an SVL (Figure 2b). Eliminating the nonadsorbed SUVs by washing and then replacing the EDTA-containing buffer with a Ca^{2+}-containing one typically resulted in the formation of single-bilayer disks (Figure 2c).[24] A continuous SPB could be obtained if Ca^{2+} was added without washing and if the surface density of vesicles in the SVL was sufficient (not shown). SUVs prepared in EDTA-containing buffers at lipid concentrations in excess of ~1 mg/mL gave rise to SPBs (not shown).

Qualitatively, higher NaCl concentrations favored vesicle adsorption to mica. Otherwise identical behavior was observed for all NaCl concentrations tested (Table 2).

An SPB was formed on mica from SUVs prepared in Ca^{2+}-containing buffers at lipid concentrations larger than ~0.25 mg/mL. Intact vesicles could be observed at lower lipid concentrations (e.g., ~10 μg/mL) used in time-resolved studies of SPB formation described below. On silica, no effect of Ca^{2+} on SPB formation from SUVs was observed, consistent with the literature concerning zwitterionic phospholipids (Table 1).

EUVs, Extruded through 30 or 50 nm Pore Diameter Filters ($R \sim 15$, $R \sim 25$ nm). EUVs (up to 3 mg/mL, the highest lipid concentration investigated) composed of EggPC adsorbed to mica intact in EDTA-containing buffer (Figure 2d). To exclude the possibility that a bilayer was formed on mica underneath the vesicles shown in Figure 2d, CTB_5 was added to the preparation. The mica surface became covered with CTB_5, and most, but not all, of the vesicles were displaced, indicating that the mica surface underneath the vesicles was not covered with an SPB (Figure 2e). It is therefore concluded that EUVs with $R \sim 15$ and 25 nm do not give rise to SPBs in the absence of Ca^{2+}.

In the presence of Ca^{2+}, continuous SPBs were observed at concentrations as low as ~0.1 mg/mL. Disks were found

(19) Rädler, J.; Radmacher, M.; Gaub, H. E. *Langmuir* **1994**, *10*, 3111.

(20) Mou, J.; Yang, J.; Shao, Z. *J. Mol. Biol.* **1995**, *248*, 507.

(21) Sixma, T. K.; Pronk, S. E.; Kalk, K. H.; Wartna, E. S.; van Zanten, B. A. M.; Witholt, B.; Hol, W. G. J. *Nature* **1991**, *351*, 371.

(22) Yeager, P. L. *The Membranes of Cells*, 2nd ed.; Academic Press: San Diego, CA, 1987.

(23) *E. coli* lipids are composed of ~85% phosphatidylethanolamine, 10% phopshatidylglycerol, and 5% cardiolipin. Both PG and CL are negatively charged.

(24) It should be noted that addition of Ca^{2+} in this case is asymmetric with respect to the bilayer and will not be considered in detail. The effects of Ca^{2+} on SPB formation discussed below refer to its presence on both sides of the bilayer.

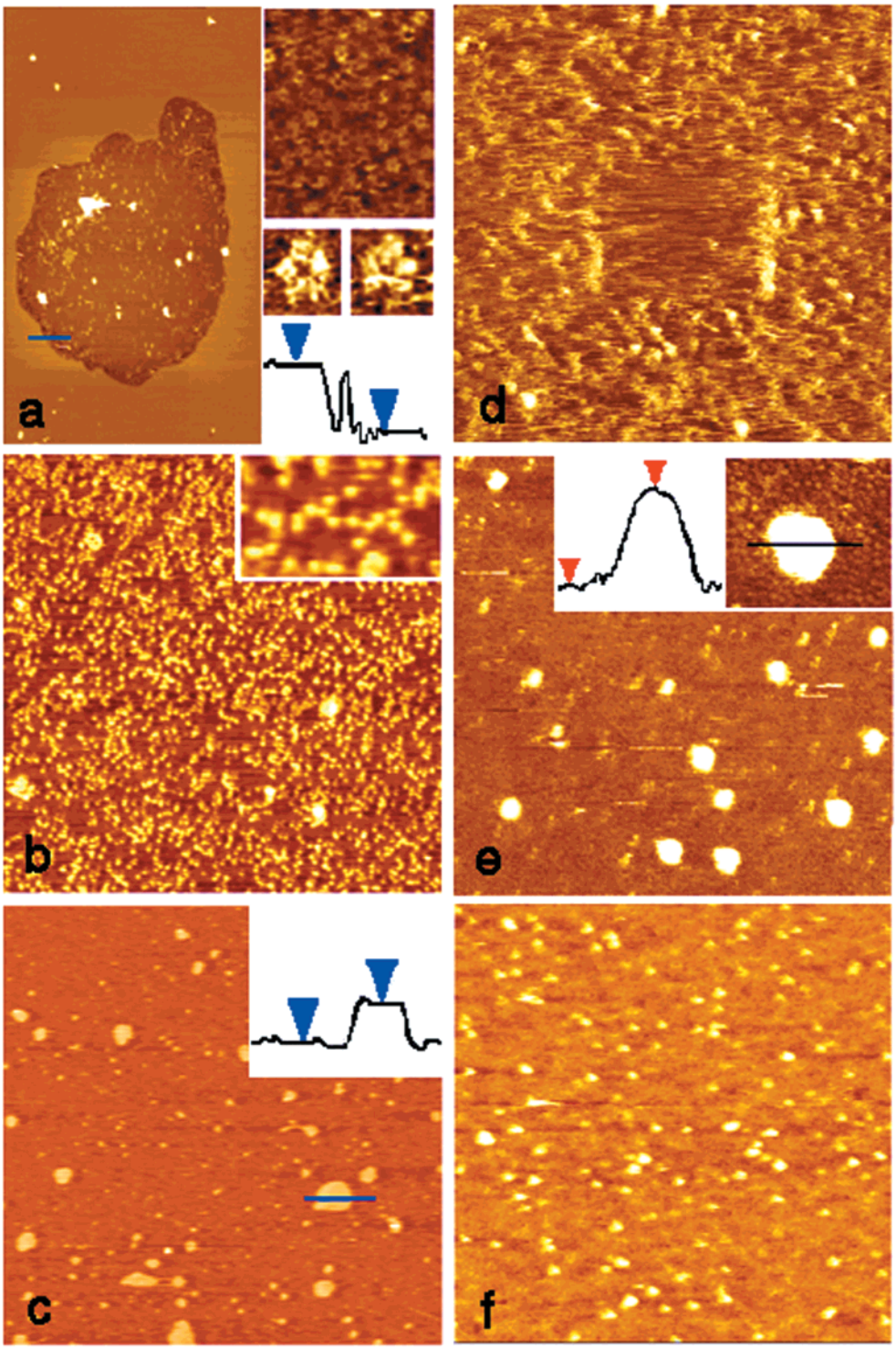

Figure 2. (a) CTB_5 molecules covering a defectuous area in an SPB. Image size: 1.8 μm. *Z*-scale, black-to-white: 0−10 nm. Top inset: 20× magnified view of an area from within the defect, showing the close-packed arrangement of annular-shaped CTB_5 molecules ~6 nm in size. Middle inset: high-magnification views of two CTB_5 molecules adsorbed on mica, in which the five constituting B-subunits and the ~1 nm-wide central opening are resolved. Bottom inset: height profile measured along the blue line showing that the SPB surface is 1.3 nm higher than the top of the CTB_5 molecules.[20,21] (b) SUV, prepared in buffer 5 at 0.5 mg/mL lipid, adsorbed on mica. Image size: 1.5 μm. *Z*-scale: 15 nm. Inset: 2.6× magnified view of an area within the image. (c) After eliminating the nonadsorbed SUVs by washing and then replacing EDTA-containing buffer (buffer 5) with a Ca^{2+}-containing one (buffer 4), adsorbed SUVs give rise to single-bilayer disks. The height of the disks (inset, measured along the blue line) is ~4 nm above the mica surface. Their size is clearly larger than would be expected from the size of SUVs shown in part b, indicating that more than one liposome participated in the formation of a disk. Scan size: 7.8 μm. *Z*-scale: 50 nm. (d) EUVs, extruded through 50 nm filters adsorb to a mica surface in the absence of Ca^{2+} (3 mg/mL lipid, buffer 5). Individual vesicles are not discernible within the aggregate. An area with some material removed during previous scans is visible in the center of the image. Image size: 1.5 μm. *Z*-scale: 15 nm. (e) Sample shown in part d, after addition of CTB_5. Most of the vesicles have been displaced from the mica surface. Image size: 0.75 μm. *Z*-scale: 8 nm. Right inset: a 100 × 110 nm^2 area showing a vesicle surrounded by CTB_5 molecules. The height of the vesicle above the CTB_5 (left inset) was measured along the black line and found to be ~5 nm. *Z*-scale: 5 nm. (f) $R \sim 15$ nm EUVs, prepared in buffer 4 at ~4 μg/mL, adsorbed to the mica surface. CTB_5 had to be added to the sample in order to obtain an image with discernible individual vesicles. Scan size: 870 nm. *Z*-scale: 50 nm.

at lower lipid concentrations (~10 μg/mL), the sizes of which were found to increase with the lipid concentration. Decreasing the lipid concentration by another factor of 10 allowed intact 30 nm EUVs to be observed (Figure 2f).

EUVs, Extruded through 100 nm Pore Diameter Filters ($R \sim 50$ nm). Both single-bilayer disks and vesicles could be visualized by AFM when 100 nm EUVs (~6 μg/mL) prepared in EDTA-containing buffer were allowed to adsorb to mica (Figure 3a). Single-bilayer disks had a constant height of 5 ± 1 nm above the mica and varied in size, while vesicles varied in size as well as height (Figure 3b). Size distributions for both types of objects are shown in Figure 3c and d, respectively. The mean radius of adsorbed vesicles was found to be 41−50 nm (Figure 3c), while that of disks was 142−160 nm (meaning that the mean radius of the vesicles, which gave rise to the disks, was 71−80 nm; Figure 3d). Increasing the concentration (or the amount) of lipid led to the formation of larger disks and ultimately of a continuous SPB.

The behaviors of 100 nm diameter vesicles prepared in Ca^{2+}-containing buffer were found to be similar. However, the quality of the images obtained at low lipid concentrations was not sufficient to ascertain whether vesicles coexisted with disks under these conditions.

EUVs, Extruded through 200 nm Pore Diameter Filters ($R \sim 100$ nm). No intact vesicles were observed with 200 nm EUVs prepared in EDTA-containing buffer (buffer 5, data not shown). Single-bilayer disks were found instead, indicating that the vesicles adsorbed to the mica surface and ruptured. The radius of the disks was consistent with the liposome size. Vesicles behaved in a similar fashion in the presence of Ca^{2+}, except an SPB was observed at lower lipid concentrations (Table 2). Lipid aggregates, which could not be removed by gentle washing, were observed on the surface of the bilayer.

Formation of an SPB Investigated by Time-Resolved AFM. Time-dependent sequences of images were acquired in an attempt to gain further understanding of the process of SPB formation from SUVs. A suspension of EggPC SUVs at a lipid concentration of ~0.8 μg/mL in a Ca^{2+}-containing buffer was circulated through the fluid cell of the atomic force microscope. Under these conditions, the adsorption of intact vesicles (Figure 4b,c) preceded the formation of bilayer disks (Figure 4d,e).

Vesicles with radii larger than those of SUVs (an arrow in Figure 4d) were consistently observed in these time-dependent experiments. Their appearance coincided with the appearance of disks if the SUV suspension was perfused through the fluid cell continuously (method i). If, on the other hand, the SUV suspension was injected into the fluid cell 0.1 mL at a time (method ii), their appearance preceded the appearance of disks, suggesting that fusion between surface-bound vesicles had occurred.[25]

Effect of AFM Tip on the SPB Formation. It is well established that the tip exerts significant (lateral) forces on the sample when the atomic force microscope is operated in contact mode. While precautions were taken in this study to reduce tip-induced artifacts as much as possible by increasing the scan rate[19] and decreasing the normal force, some artifacts were observed. In particular, it is clear from the image shown in Figure 5 that the area of the (incompletely formed) bilayer which was scanned

(25) The difference between the two methods—i and ii (see Experimental Section)—is due to the fact that the former does not necessarily represent the equilibrium situation, while the latter one does. The significance of these vesicles and of whether the system is in equilibrium or not is elaborated on in the Discussion.

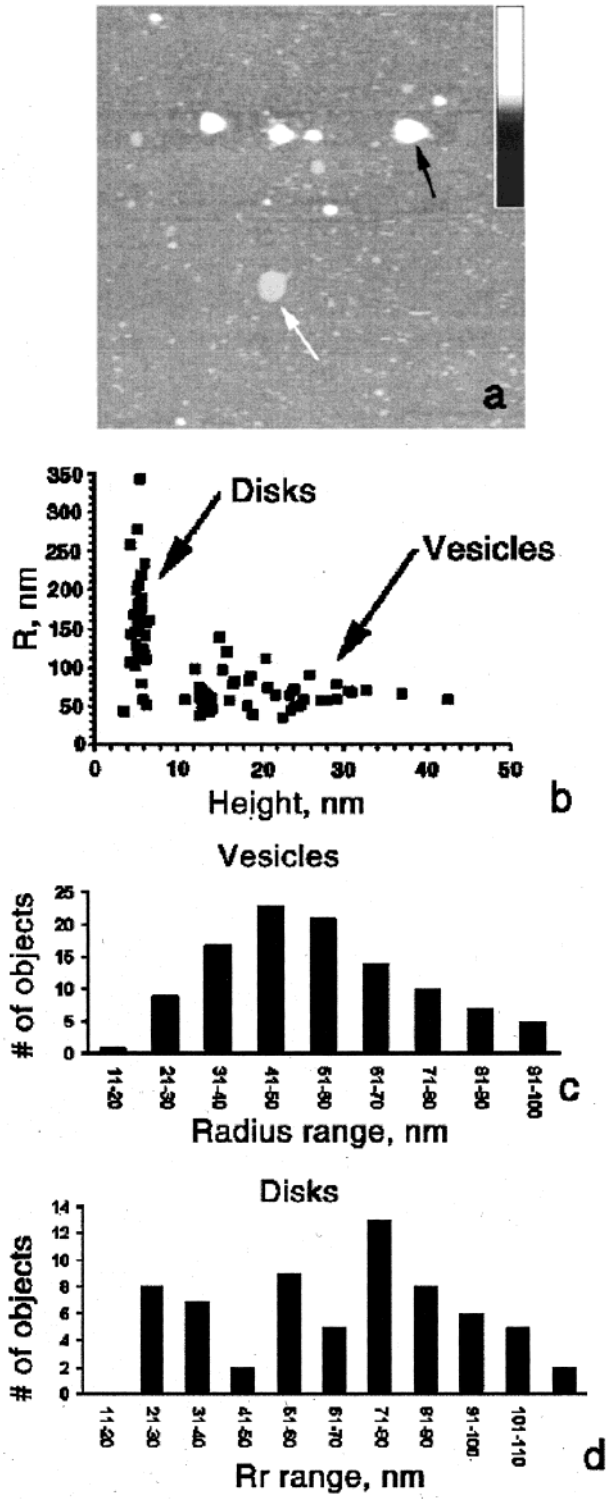

Figure 3. (a) Incubation of $R \sim 50$ nm EUVs prepared in buffer 5 on mica results in single-bilayer disks (white arrow) as well as vesicles (black arrow) being present. To increase the image quality, CTB_5 was added to the preparation before this image was acquired; however, the size distribution analysis was performed in the absence of CTB_5 to avoid artifacts. Scan size: 3.2 μm. *Z*-scale, black to white: 0−75 nm. (b) Radius versus height plot of the objects (disks and vesicles) found on images such as the one shown in part a. Disks have a nearly constant height of ~5 nm and vary in size, while vesicles vary significantly in height.[26] (c and d) Size distributions of vesicles and disks, respectively. For the disks, the equivalent radius of the vesicle is quoted: a vesicle with radius 60 nm would give a disk with a radius of 120 nm.

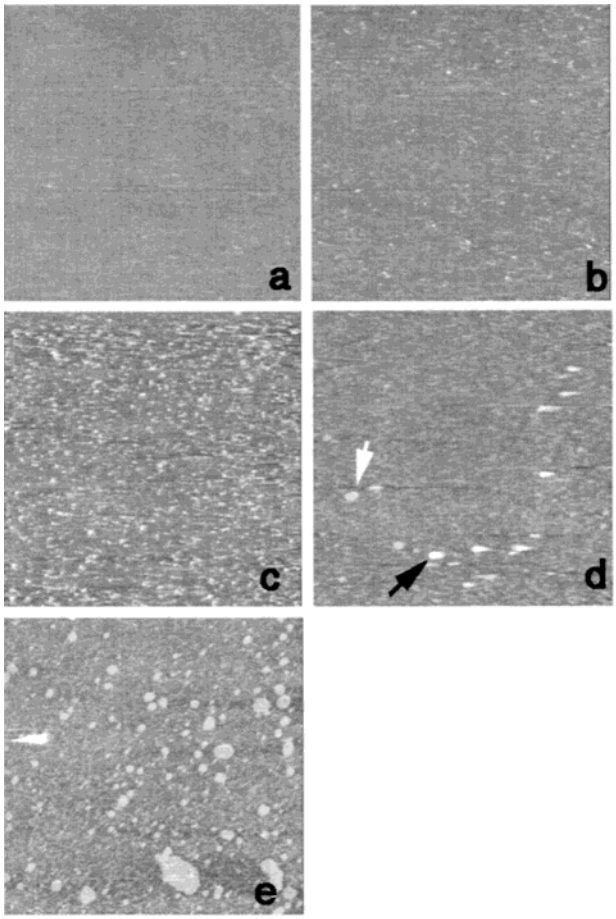

Figure 4. Time-lapse sequence of the early stages of SPB formation. A 0.8 μg/mL EggPC SUV suspension in buffer 4 was perfused through the fluid cell using a syringe pump. Amount of lipid perfused through the cell: (a) 0 μg; (b) 0.06 μg; (c) 0.2 μg; (d) 0.8 μg. The onset of disk formation is observed (white arrow). The black arrow points to a vesicle which is thought to have arisen through fusion of surface-bound vesicles (see text). (e) 2.3 μg. For comparison, ~0.5 μg is required to completely cover a 12 mm mica disk with an EggPC bilayer (assuming the surface area covered by one EggPC molecule to be 62 Å^2 [22]). Image size (*Z*-scale): (a, b, c) 5 μm (15 nm); (d and e) 10 μm (50 nm).

repeatedly differs in the size and the number of defects from the area outside. A similar trend can be seen in Figure 4d.

Discussion

Before discussing the mechanism of SPB formation from unilamellar vesicles implied by the results presented above, an important point concerning the distinction between single-bilayer disks and adsorbed vesicles has to be addressed. Single-bilayer disks (Figures 2c, 3a, 4d,e) and adsorbed vesicles (Figures 2b–f, 3a, 4b,c) differ in their appearance on the AFM images as well as in their behavior with respect to the addition of CTB_5 or Ca^{2+}: First, disks exhibited a constant height of ~5 nm (Figure 3b), while the height of the adsorbed vesicles varied.[26] Second, CTB_5 was found either to displace the adsorbed vesicles and cover the surface completely or to coexist with the (larger) adsorbed vesicles (Figures 2e,f, 3a). CTB_5 was never observed to displace bilayer disks. Finally, the addition of Ca^{2+} transformed vesicles into disks (Figure 2c).[24] These differences allowed the two types of objects to be distinguished from each other. However, it is not possible to determine by AFM whether the vesicles observed are truly "intact", that is, whether the integrity of the bilayer has changed during adsorption—a phenomenon which may be relevant for the fusion between surface-bound vesicles (see below). To the best of the authors' knowledge, there has been no published study addressing this latter issue.

(26) There are two likely reasons for the variability in the apparent height of vesicles above the mica and for the unreasonably low absolute values of the height. First, the surface-bound vesicles may move during imaging—an explanation supported by the fact that the height of the vesicles above CTB_5 was more consistent (see figure legends). (The height of biological macromolecules as measured by AFM is discussed in ref 48). Second, vesicles are soft objects and are likely to be deformed by the tip during imaging.

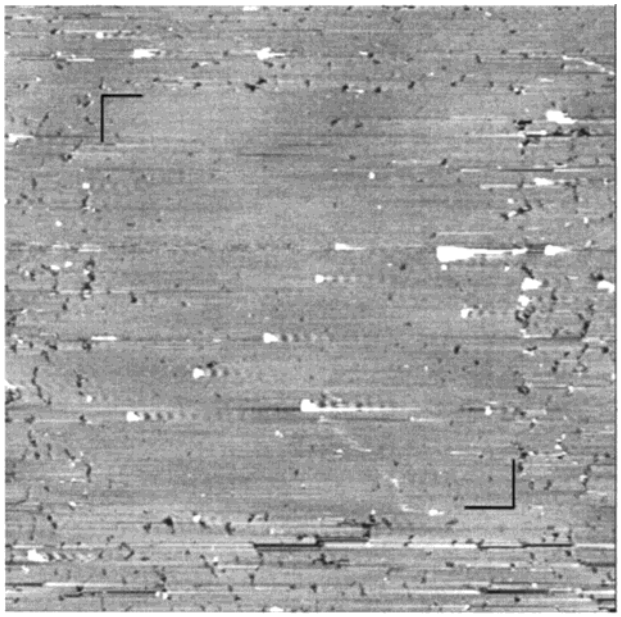

Figure 5. Effect of the AFM tip on the formation of an SPB. The late stages of SPB formation were followed in time after injection of 0.02 mg/mL EggPC SUVs in buffer 4 into the fluid cell. The relatively defect-free 10 × 10 μm^2 area outlined with black corners was repeatedly scanned (at the lowest possible normal force). Image size: 1.5 μm. *Z*-scale: 15 nm.

Mechanism of SPB Formation from Unilamellar Vesicles. It is convenient to consider the formation of a supported phospholipid bilayer on a solid surface from vesicles present in solution as a sequence of the following stages: Initially, vesicles adsorb to the surface. The adsorbed vesicles may subsequently rupture or may fuse with each other before they can rupture. In either case, single-bilayer disks are formed, which will then grow and coalesce to form a continuous SPB. The initial stages of this process—adsorption, fusion, and rupture—have been investigated theoretically by Seifert and Lipowsky.[13,14] The observations comprising this report will now be discussed in terms of their theoretical model. For the sake of simplicity, the results obtained in the absence of Ca^{2+} will be discussed first and the effect of Ca^{2+} will be considered separately.

Vesicle Adsorption. Under the conditions where an SPB was formed, the adsorption of intact vesicles preceded the formation of an SPB, as shown by the time-resolved experiments and the experiments investigating the effect of lipid concentration on SPB formation (see also Keller et al.[9,10]). We shall therefore start by considering the adsorption of vesicles (Figure 6a).

Adsorption of a vesicle to an attractive wall is governed by the interplay between the (favorable) adhesion energy and the (unfavorable) bending energy.[13,14] The former is the energy gained by the vesicle upon adhering to the

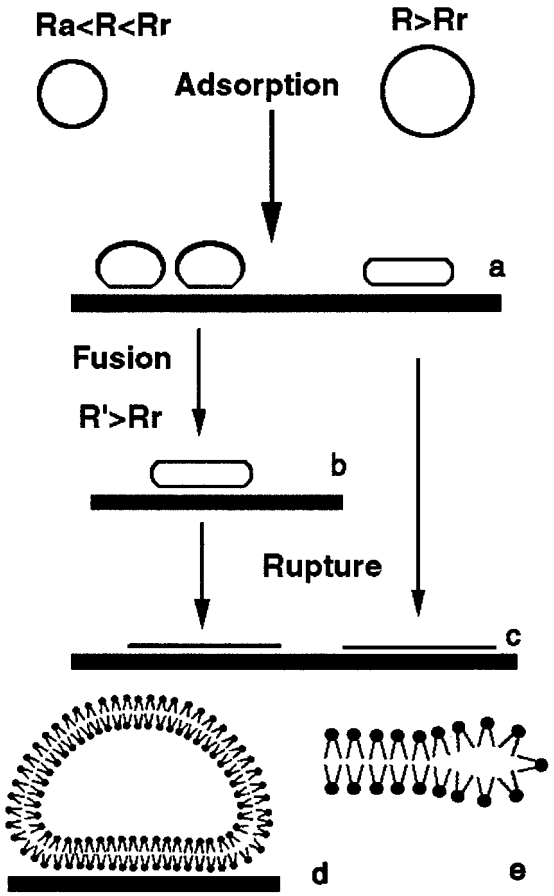

Figure 6. Model of the early stages of SPB formation. (a) Vesicle adsorption to a solid surface (black). At large R and/or W, an adsorbed vesicle resembles a pancake. The structure of an adsorbed vesicle of lower radius or at lower potential is schematically depicted in part d. (b) Fusion of surface-bound vesicles leads to an increase in the vesicle radius. Consequently, the adsorbed vesicle becomes more pancake-like and ruptures. (c) Rupture of surface-bound vesicles with $R > R_r$ leads to the formation of single-bilayer disks. Two possible structures of the "active edge" are schematically depicted in part e. R, vesicle radius. R_a and R_r have the same meaning as in the text (see also Appendix I).

wall and is expressed as $F_a = -WA^*$ (A^* is the contact area, and W is the effective contact potential).[13,14] It increases with the size of the vesicle. The latter, expressed as $F_b = {}^1/_2 k \int dA(C_1 + C_2)^2$ (where k is the bending rigidity of the bilayer, C_1 and C_2 are the two principle curvatures, and the integration is performed over the surface area A of the vesicle),[27] results from the deviation of the vesicle from a spherical shape (bending) upon adhesion and depends on the bending modulus of the membrane k but not on the vesicle size. Therefore, for a given W, the gain due to the size-dependent adhesion energy becomes higher than the cost due to the size-independent bending energy when the size of the vesicle R is larger than the critical radius R_a:[13,14]

$$R_a = (2k/W)^{1/2} \tag{1}$$

The size distribution of bound vesicles is therefore expected to exhibit a lower cutoff at a this critical radius as long as the experimental time scale is sufficiently long compared to the time required to attain zero pressure difference between the inside and the outside of the vesicle (i.e., for water to permeate through the membrane). The fact that the SUVs remained adsorbed to the mica surface for extensive periods of time (hours) indicates that for the case of mica under the conditions used in this study, the cutoff radius R_a lies below the radius of the SUVs. SUVs represent the vesicles of the smallest attainable size (~12 nm[22]), which therefore places an upper limit on R_a in the absence of Ca^{2+} as well as in its presence (discussed below). The situation with silica seems to be similar.[9,10]

Formation of Disks by Rupture of Adsorbed Vesicles. With respect to the formation of disks from adsorbed vesicles (Figure 6c), the energy of the initial state (a bound vesicle, which in the limit of large R and/or W becomes flattened and resembles a pancake) has to be compared with that of the final state (a bound disk). After Seifert:[13]

$$F_{bv} = -2\pi WR^2 + 2\pi g(2kW)^{1/2}R \tag{2}$$

$$F_{bd} = -4\pi WR^2 + 4\pi\Sigma R$$

where F_{bv} and F_{bd} are the free energies of the bound vesicle and disk, respectively, R is the radius of the vesicles (disks radius $R_d = 2R$), Σ is the line tension along the circumference of the disk,[28] and g is a numerical constant. A bound vesicle will rupture if $F_{bd} < F_{bv}$, which leads to an expression for the rupture radius

$$R_r = [2\Sigma - g(2kW)^{1/2}]/W \tag{3}$$

Isolated vesicles with $R \geq R_r$ will rupture while isolated vesicles with $R < R_r$ will remain intact.[13,14] We observed that, in the absence of Ca^{2+}, isolated vesicles with $R \sim$ 12,[22] 15, and 25 nm remained intact on the mica surface (Figure 2b,d,e). Both vesicles and disks coexisted on the surface when $R \sim 50$ nm was used (Figure 3a,b), indicating that vesicles with both $R \geq R_r$ and $R < R_r$ were present in the distribution. A value of $R_r \sim 75$ nm was estimated from the size distributions of vesicles and disks shown in Figure 3c,d in the absence of Ca^{2+} (see Appendix II). Finally, only disks were found with $R \sim 100$ nm EUVs, indicating that most or all of the vesicles in suspension had a radius larger than the rupture radius R_r.[29]

Fusion of Surface-Bound Vesicles. So far, two steps in the mechanism of SPB formation have been considered—that is, the adsorption of intact vesicles with $R_a < R$ and the rupture of adsorbed vesicles with $R \geq R_r$ to form single-bilayer disks. The third step—namely, that of fusion of surface-bound vesicles (Figure 6b)—needs to be introduced for interpreting the observations with SUVs ($R \ll R_r$)[30] as well as EUVs in the presence of Ca^{2+}.

It was demonstrated theoretically that adhesion of vesicles to a surface favors their fusion.[13,14] The change

(27) Helfrich, W. Z. *Naturforsch* **1973**, *28c*, 693.

(28) The structure at the edge of the disk is not known. It is usually assumed that the hydrophobic core of the bilayer is exposed to the aqueous environment at what is referred to as the "active edge" (cf. Figure 6e). Σ can then be calculated from the interfacial tension of tetradecane in water (52 mJ/m^2 [49]) multiplied by the thickness of the hydrophobic segment of the bilayer (~2.5 nm), which gives $\Sigma = 1.3 \times 10^{-7}$ mJ/m.

(29) It should be noted that an SPB can be formed from a vesicle suspension with a mean radius smaller than R_r, as long as this suspension contains vesicles with radii larger than R_r. They will form single-bilayer disks. An intact vesicle adsorbed in close proximity to the "active edge" of such a single-bilayer disk will fuse with it (see the discussion of the late stages of SPB formation below). At high enough lipid concentrations, this process will lead to the formation of an SPB.

(30) At the low lipid concentrations and small time scales involved in the current study, fusion of SUVs and—especially—EUVs in solution is considered to be unlikely.

in energy associated with the fusion of two bound vesicles[31]

$$\Delta F_{bv} = \text{const} \times (kW)^{1/2}R + 4\pi k_g \qquad (4)$$

where k_g is the bending modulus associated with the Gaussian curvature of the bilayer,[32] should be positive for fusion to be favored.[14] Therefore, at given values of k, W, and k_g, vesicles with radii smaller than some radius R_f will be stable, while the larger vesicles will fuse.

Evidently, in the absence of Ca^{2+}, fusion of surface-bound EUVs with $R < R_r$ does not occur. The stability of EUVs in the absence of Ca^{2+} can be used to estimate the lower limit on R_f: ~75 nm (see Appendix II). This value leads to quite a reasonable estimate of the k/k_g ratio for a phospholipid bilayer (see Appendix II).

The formation of an SPB from SUVs, the radii of which are smaller than those of EUVs, at sufficiently high lipid concentrations implies that fusion has occurred between surface-bound SUVs. This difference in behavior between SUVs and EUVs at constant W must be associated with the properties of the bilayer (described by the values of k and k_g) being different in the cases of EUVs and SUVs. Indeed, the number of phospholipid molecules in the inner leaflet of the SUVs is significantly smaller than that in the outer one. Intuitively, this should oppose bending and make the bilayer stiffer, which, according to eq 4, would favor fusion. Bearing in mind that, even in solution, SUVs represent thermodynamically unstable, kinetically trapped species and that adsorption facilitates fusion of vesicles,[13,14] the above explanation is not unreasonable.

It should be noted that, according to Seifert and Lipowsky,[13,14] the second term in eq 4 can be ignored in the limit of very large R and/or W, where an adsorbed vesicle resembles a pancake. This would imply that fusion is favored for surface-bound vesicles of all sizes, under all conditions—a picture incompatible with the observations presented in this report. Therefore, under the conditions investigated here an intermediate regime is encountered: R and/or W are large enough for an adsorbed vesicle to resemble a pancake but not large enough for the second term in eq 4 to be ignored. On the other hand, it is also necessary to point out that the barriers to fusion may be kinetic, and not thermodynamic, in nature.

To summarize the preceding discussion, in the absence of Ca^{2+}, vesicles of all sizes investigated here adsorb to mica. While surface-bound SUVs were found to undergo fusion in the absence of Ca^{2+}, EUVs were found to be stable. Therefore, in the absence of Ca^{2+}, SPBs could be formed only from suspensions containing vesicles with $R \geq R_r$, and from SUVs.

Effect of Ca^{2+} on the Formation of an SPB from Zwitterionic Phospholipids on Mica. The results presented in this report indicate that Ca^{2+} enhances the SPB formation process. In the presence of Ca^{2+}, SPBs formed from vesicles of all sizes investigated. Furthermore, there is direct, as well as indirect, evidence for the fusion of surface-bound vesicles in the presence of Ca^{2+}: The former comes from the time-resolved experiments with SUVs in the presence of Ca^{2+} (Figure 4d; see Results), while the latter comes from the fact that the size of single-bilayer disks formed from 30 nm EUVs increased with the lipid concentration (see Results).

As was already mentioned in the section concerning vesicle adsorption, R_a remains below ~12 nm in the presence of Ca^{2+}. Only a lower limit of ~15 nm can be placed on R_r ($R_r > 15$ nm in the presence of Ca^{2+}, Figure 2f), owing to the poor quality of images obtained in the presence of Ca^{2+} and rather low lipid concentrations required to observe individual vesicles. Therefore, there is a strong possibility that Ca^{2+} affects the effective interaction potential W and, consequently, R_a, R_r, and the critical fusion radius R_f, which changes from above 75 nm to below 15 nm. However, the restriction on W set out above by the value of R_r is incompatible with such a change in R_f at constant k and k_g (see Appendix II). Therefore, proceeding within the framework of Seifert and Lipowsky's model, we propose that Ca^{2+} modifies the bending moduli k and k_g of the bilayer. Thus, the same mechanism which accounts for the difference in behavior between SUVs and EUVs in the absence of Ca^{2+}, outlined in the previous section, is proposed to account for the stability of SUVs and EUVs with diameters ~30−50 nm with respect to fusion in the absence of Ca^{2+} (Figure 2b−e) and lack thereof in its presence.

The fusogenic activity of Ca^{2+} with respect to vesicles containing negatively charged phospholipids is due to its ability to mediate the formation of trans-bilayer complexes between them[11,33,34] and to induce lateral phase separation in bilayers containing mixtures of zwitterionic and negatively charged phospholipids.[35,36] A similar effect of Ca^{2+}—a phase separation in EggPC (but not DOPC) lamellar phases—has been described.[37] However, it is not clear whether this effect would be relevant here, for it is normally observed at somewhat higher Ca^{2+} concentrations than those used in this study (approximately ten times higher). Furthermore, DOPC and EggPC were found to behave identically in the current study (Table 2). No evidence of Ca^{2+}-mediated trans-bilayer complexes between zwitterionic phospholipids has been presented to date.

To summarize the preceding discussion, while the exact nature of the effect Ca^{2+} exerts remains obscure, a prominent possibility has emerged that a change in the bilayer properties is brought about by Ca^{2+} binding, which leads to fusion of otherwise stable vesicles—a possibility which shall be revisited in the subsequent section.

Late Stages of SPB Formation: Fusion of Vesicles with Single-Bilayer Disks. A Consistent View of the Driving Forces Involved in Fusion of Surface-Bound Vesicles and of the Effect Ca^{2+} Exerts on this Process. At low concentrations of vesicles in the bulk, the growth of isolated domains ceased after some time. Individual domains did not coalesce into one larger domain but remained isolated after hours of observation (Figures 2c and 4d,e), indicating that the single-bilayer disks do not move on the surface or at least do so extremely slowly. Addition of fresh vesicles into the fluid cell of the atomic force microscope resulted in further growth (not shown). A sequence of images capturing the late stages of SPB

(31) It is intuitively clear that this process will also depend on the lipid concentration, since higher concentrations increase the probability of contact between vesicles. In fact, this is the only step in the formation of single-bilayer disks (adsorption of vesicles, their fusion, disk formation by vesicle rupture) which is concentration-dependent. However, the definition of "contact" is not trivial in this case, and it is therefore difficult to take the concentration dependence into account.

(32) To the best of the authors' knowledge, k_g has neither been measured nor estimated for bilayers although experimentally determined values for monolayers exist.[47] In general, it is thought to be negative.[47]

(33) Wilschut, J.; Düzgünes, N.; Papahadjopoulos, D. *Biochemistry* **1981**, *20*, 3126.

(34) Day, E. P.; Kwok, A. Y. W.; Hark, S. K.; Ho, J. T.; Vail, W. J.; Bentz, J.; Nir, S. *Proc. Natl. Acad. Sci. U.S.A.* **1980**, *77* (7), 4026.

(35) Leckband, D. E.; Helm, C. A.; Israelachvili, J. *Biochemistry* **1993**, *32*, 1127.

(36) Helm, C. A.; Israelachvili, J. N.; McGuiggan, P. M. *Science* **1989**, *246*, 919.

(37) Lis, L. J.; Lis, T. W.; Parasegian, V. A.; Rand, R. P. *Biochemistry* **1981**, *20*, 1771.

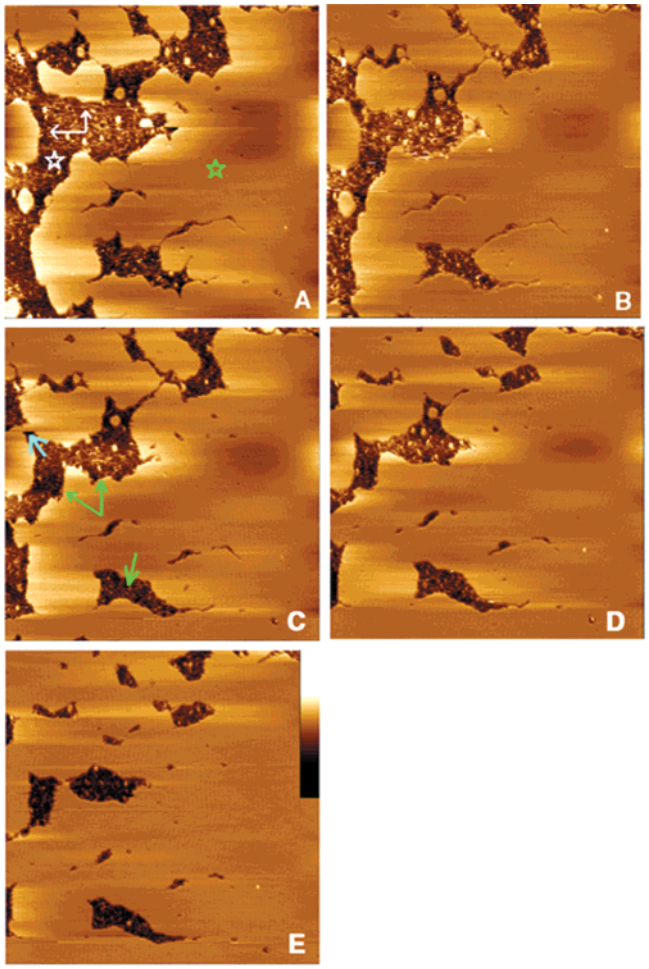

Figure 7. Late stages of SPB formation from EggPC SUVs. Time after onset of imaging: (A) 6 min; (B) 14 min; (C) 23 min; (D) 30 min; (E) 54 min. (A) Part of the mica surface (white star) is covered by lipid debris, originating from spread SUVs and their aggregates. Planar lipid domains (green star) cover most of the mica surface. The two white arrows point to two characteristic lipid domains, which will grow and coalesce from part A to part E. In part C, a connection has been established between them (blue arrow). Some mica areas stay devoid of a SPB (green arrows). The consistent darker aspect, and thus lower level, of these defectuous areas indicates that less lipid material is adsorbed locally. Scan size: 3 μm. *Z*-scale (shown in part e), from black to white: 10 nm.

formation—from lipid domains of various sizes already formed on the mica to a uniformly flat, nearly continuous SPB—is shown in Figure 7. It has been proposed that, in the case of SUVs, the formation of SPBs results from the advancement of single bilayers with open edges and that this process results in incomplete coverage.[2] Our results indicate that SPBs do form via coalescence of edge-active single-bilayer domains, which grow by incorporating lipids from vesicles adsorbed in their immediate vicinity, but that this process results in an (almost) complete surface coverage.[38] To understand why this is the case, we must consider in detail the process of fusion of an adsorbed vesicle with an active edge presented by a single-bilayer disk (or, which is equally important, by a defect in a bilayer)—the process which, as we shall see, is directly related to the fusion of surface-bound vesicles discussed above.

Irrespective of whether the hydrophobic portion of a bilayer is exposed at the edge of a single-bilayer disk[28] or a spherical "cap" is present at the edge of a domain (Figure 6e),[39] the hydrophobic segments of the acyl chains will be exposed to the aqueous environment. The fusion of an adsorbed vesicle with a disk is therefore driven by the hydrophobic effect, in a fashion identical to that of fusion between depleted or phase-separated supported phospholipid bilayers.[35,36] Furthermore, let us suppose that an adsorbed vesicle has packing defects at its edges (Figure 6d) due to bending. It then becomes apparent that the fusion of two adjacent surface-bound vesicles and the fusion of an adsorbed vesicle with an adjacent disk are manifestations of the same process. The extent to which a given potential W can deform the bilayer—that is, whether such packing defects will or will not be present—depends on the bending moduli k and k_g of the latter. We therefore return to the previously introduced idea that it is the difference in the properties of the bilayer (i.e., the bending moduli) that is responsible for the different behavior of SUVs and EUVs in the absence of Ca^{2+}. Extending the above argument one step further brings us to the possibility that Ca^{2+} modifies the bending moduli (via modifying the packing of the phospholipids), increasing the extent of the deformation possible upon adsorption and therefore promoting fusion. It is important to bare in mind that this effect need not be apparent in bulk, for the properties of the Ca^{2+} binding sites on the bilayer of the free vesicles are likely to be different than those of the adsorbed ones. Therefore, the effect of Ca^{2+} may be exerted locally. It is furthermore important to realize that, in the theoretical model of Seifert and Lipowsky, the membrane is considered as a thin flexible sheet and the molecular details of its structure are ignored—while fusion of vesicles involves bilayer properties associated with its discrete, molecular structure.

Fusion of vesicles with the domains' edges will result in expansion of the domains. Figure 7 faithfully illustrates this process. Since vesicles are also free to fuse with defects in the bilayer, eventually a continuous SPB will be formed.

Effect of AFM Tip on the SPB Formation. It is evident from Figure 5 that the tip acts as a localized stirrer, ensuring a steady supply of building material for the growing domains, increasing the average domain size, and reducing the number of defects in the area which is scanned repeatedly. This type of tip-induced artifact predominantly affects the kinetics of the processes which occur on the surface. This makes obtaining quantitative information on the rate of domain growth somewhat difficult. (It is not at all clear whether tapping mode AFM would be free of such an artifact, for an oscillating cantilever can cause the same effect).

SPBs Containing Receptor Molecules for Membrane-Binding Proteins. One of the major attractions of SPBs to a biophysicist is the ability to investigate macromolecules bound to SPBs containing appropriate receptor molecules. Such systems are suitable for investigation by AFM, ATR-FTIR, SPR, and so forth—methods otherwise not applicable to the study of protein–lipid interactions. Nearly defect-free[38] bilayers incorporating up to 10% G_{M1} or 0–80% DOPS in mixtures with DOPC or DPPC[40] can be obtained on mica by fusion of unilamellar vesicles in Ca^{2+}-containing buffers (see Tables 1 and 2; cf. and refs 15, 20, 41, 42). Ternary mixtures thereof can also be used to prepare SPBs. Images of CTB_5 bound to G_{M1}-

(38) Remaining (small) defects are thought to be due to the local properties of mica. See also ref 20.

(39) Rinia, H. A.; Demel, R. A.; van der Eerden, J. P. J. M.; de Kruijff, B. *Biophys. J.* **1999**, *77*, 1683.

(40) Reviakine, I.; Simon, A.; Brisson, A. *Langmuir*, in press.

(41) Mou, J.; Yang, J.; Huang, C.; Shao, Z. *Biochemistry* **1994**, *33* (3), 9981.

(42) Fang, Y.; Yang, J. *Biochim. Biophys. Acta* **1997**, *1324*, 309.

containing SPBs are familiar to the bio-SPM community.[15,20] Recently, DOPS-containing SPBs have also been used to support the growth of 2D crystals of Annexin V.[17,40,43]

Conclusions and Further Work

To summarize, we found that isolated vesicles adsorb to mica intact as long as their radii are smaller than the rupture radius (R_r), while vesicles of larger size rupture and form single-bilayer disks. This is schematically shown in Figure 6a,c. Vesicles of all sizes investigated here were found to adsorb to mica, indicating that the critical adsorption radius R_a below which vesicles no longer adsorb to the surface[13,14] could not be observed in our system.

Fusion of surface-bound vesicles predicted by Seifert and Lipowsky[13,14] was observed in the presence of Ca^{2+}, while in its absence surface-bound extruded vesicles with $R \sim 15$ and 25 nm were found to remain intact at all lipid concentrations tested (up to 3 mg/mL). On the other hand, sonicated unilamellar vesicles gave rise to SPBs in the absence as well as in the presence of Ca^{2+}, but a higher lipid concentration was required in the former case than in the latter. The difference in behavior of SUVs and EUVs is attributed to the different properties—the bending moduli—of the bilayers in the two cases. It is proposed that Ca^{2+} promotes fusion by modifying, perhaps locally, the properties of the bilayer.

Continuous adsorption of vesicles from solution leads to the growth of single-bilayer disks and their coalescence, while isolated disks remain intact and immobile (cf. ref 2) if vesicles are not present in the subphase.

The mechanism of SPB formation on silica proposed recently by Keller et al.[9,10] correlates well with the one identified in this report on mica.

Further work is clearly required to achieve a quantitative description of the process of SPB formation and to understand the role played by ions—like Ca^{2+}—in this process. Furthermore, the effects of various preparation methods and media compositions on an intimately related question of liposome stability deserve further experimental investigation.

Note. A paper by Egawa and Furusawa[45] appeared after our manuscript had been submitted. The authors studied SPB formation from 200 nm diameter EUVs. While their results appear to be consistent with ours, no distinction is made by the authors between the nonruptured vesicles and disks.

Appendix I: List of Symbols Used throughout the Text, with Units

C_1, C_2 = principle curvatures, 1/nm.

F_{xx} = free energy of an appropriate object, J

k = bending modulus of the bilayer, J

k_g = bending modulus associated with the Gaussian curvature of the bilayer, J

R = vesicle radius, nm

R_a = critical adsorption radius, nm. Vesicles with $R \geq R_a$ adsorb to the surface. Vesicles with $R < R_a$ do not.

R_f = critical fusion radius for adsorbed vesicles, nm. Adsorbed vesicles with $R \geq R_f$ have a tendency to fuse with each other, while vesicles with $R < R_f$ are stable.

R_r = critical rupture radius, nm. Adsorbed vesicles with $R \geq R_r$ rupture and form single-bilayer disks. Adsorbed vesicles with $R < R_r$ are stable and remain intact.

W = effective contact potential, J/m^2

Σ = line tension along the circumference of the disk, J/m

Appendix II

While the work presented above is largely qualitative in nature, some quantitative information can be extracted from our experiments. It is listed below.

First, the effective interaction potential W can be estimated from the size distribution of the surface-bound vesicles and disks shown in Figure 3. The former exhibits a peak at ~41−50 nm radius (Figure 3c), and the latter exhibits one at ~71−80 nm (the equivalent vesicle radius is quoted, $R = {}^1/_2 R_d$; Figure 3d).[44] Thus, a value of 75 nm can be taken as a crude estimate for the rupture radius R_r. This yields a value of ~3.5 mJ/m^2 for the effective potential W in the absence of Ca^{2+} using eq 3 with $k = 3.9 \times 10^{-20}$ J or 5.8×10^{-20} J [46] and $\Sigma = 1.3 \times 10^{-7}$ mJ/m.[28] Substituting the value of W into eq 1, a value of ~5−6 nm (depending on the value of k used) is obtained for R_a.

Knowing the value of the effective potential W, a value of 117 mJ/m^2 for the area compressibility modulus of the bilayer is arrived at from the simple relation given in ref 13 (The area compressibility modulus of a bilayer is expected to be ~100 mJ/m^2 [13]).

Furthermore, from the observation that vesicles with $R < R_r = 75$ nm are stable to fusion at the potential ~3.5 mJ/m^2 in the absence of Ca^{2+}, it follows that $R_f > 75$ nm, and quite a reasonable upper limit of ~ −0.05 on the ratio of k to k_g can be arrived at (cf. ref 47) from eq 4 with the constant being equal to $4\pi g(2^{1/2} - 1)$, where $g = 2.8$.[13,14]

On the other hand, 15 nm can be taken as a lower limit on R_r in the presence of Ca^{2+}. This places an upper limit of ~10 mJ/m^2 on W (eq 3). Although it is proposed that the bending moduli are different in the presence of Ca^{2+} than in its absence, the rupture radius R_r is only weakly dependent on k, and the value of the latter in the absence of Ca^{2+} is taken as a satisfactory approximation. On the other hand, a lower limit on W cannot be calculated, since R_a strongly depends on k.

With respect to vesicle fusion, 15 nm can be taken as the upper limit on R_f in the presence of Ca^{2+}. Substituting it into eq 4 leads to a value of 85 mJ/m^2 (88 mJ/m^2) for W, keeping k and k_g as in the absence of Ca^{2+}. This value is clearly incompatible with the upper limit of ~10 mJ/m^2 worked out above.

Acknowledgment. The authors gratefully acknowledge the help of Dr. A. V. Zvelindovsky and Mr. A. N. Morozov, M.Sc., for in-depth discussions related to the theoretical aspects of vesicle adsorption and fusion, Mrs. N. Govorukhina, M.Sc., for technical assistance, Prof. J.-F. Tocanne and Dr. L. Sezanne (Toulouse, France) for allowing I.R. to visit their facility and learn the method of vesicle fusion, Dr. T. Klapwyk for the generous gift of silicon wafers, and Dr. S. Mazères for critical comments. The authors also wish to thank Dr. C. Keller (University of California, Santa Barbara) for illuminating discussions. I.R. is the recipient of a Ubbo Emmius Ph.D. fellowship from the University of Groningen. This work was supported by The Netherlands Foundation for Chemical Research (SON) and the EU (Grant B104CT96-0083 to A.B.).

LA9903043

(43) *Annexins: Molecular Structure to Cellular Function*; Seaton, B. A., Ed.; Chapman and Hall: New York, 1996.

(44) At the low lipid concentration used, fusion between surface-bound vesicles, discussed in detail above, is expected to be negligible.

(45) Egawa, H.; Furusawa, K. *Langmuir* **1999**, *15*, 1660.

(46) Niggermann, G.; Kummrow, M.; Helfrich, W. *J. Phys. II* **1995**, *5*, 413.

(47) Templer, R. H.; Khoo, B. J.; Seddon, J. M. *Langmuir* **1998**, *14*, 7427.

(48) Müller, D. J.; Engel, A. *Biophys. J.* **1997**, *73*, 1633.

(49) Israelachvili, J. *Intermolecular and Surface Forces*, 2nd ed.; Academic Press: London, 1992.

(50) Giesen, P. L. A. Production of Thrombin at Macroscopic Surfaces. Ph.D. Thesis, University of Limburg, 1992.

(51) A few (one or two) small disks could sometimes be found on samples and are thought to be due to contamination or tip-induced rupture.